Impact of Retransmission Delays on Multilayer Video Streaming over IEEE 802.11e Wireless Networks

Sai Ganesh Sitharaman and Karthik Maruthu Anantharaman
Wipro Technologies, Bangalore, India.
Email: {saiganesh.sitharaman, karthik.ananthu}@wipro.com

Abstract— **In this paper, we seek to establish probabilistic bounds of retransmission delays for transporting multilayer video frames over IEEE 802.11e QAP/QSTA with enhanced MAC distributed coordination function (EDCF). We consider an end-to-end multilayer video streaming that uses hybrid FEC/ARQ error detection and control. Under multiple priority levels of IEEE 802.11e MAC EDCF, we first establish steady-state collision probabilities and contention resolution delays, given the number of nodes. We introduce a time-varying Rayleigh slow-fading channel error model and studying its effect on MAC EDCF transmissions. For video transmissions, we model the expected waiting time of EDCF MAC video queue using Head-of-Line (HOL) priority queueing discipline using the MAC delay distribution derived earlier as service distribution. The total MAC EDCF video (base layer) queueing delay is the sum of expected waiting time of high-priority voice frames, service residual of best-effort data and the expected waiting time of video frames at HOL queue. Next, we model video retransmission events at receiver as renewal-reward process of frame(s) identified for retransmission to establish the "spread"-time between successful renewal events. The "spread"-time is indeed the probabilistic retransmission bound that we seek for a single video frame identified for retransmission. We verify our model and analytical bounds using an in-house Multimedia Mobile Communication Platform (*MMCP*), written entirely in software to study the cross-layer interworking between MAC and transport for IEEE 802.11 and 802.11e MAC. MMCP currently supports MPEG4 single-layer and FGS two-layer with concurrent voice and video streaming capabilities. Our model, when combined with a receiver-based channel feedback, can yield a jitter-free, rate-adaptive and guaranteed "base" video quality.**

Index Terms— **FEC/ARQ, Video Streaming, 802.11, EDCF.**

I. Introduction

THERE, is an increasing demand to offer multimedia voice and video services over telecommunications-based cellular packet-switched networks as well as over IEEE 802.11-based wireless LAN [11], [12]. These services are likely to adopt latest audio/video compression, coding and transportation standards. In 2003, the Joint Video Team (JVT) of ISO/MPEG and ITU-T proposed H.264/AVC Joint Video Specification that uses several new techniques to enhance video compression and transportation. Higher video compression is achieved through variable block-size motion compensation, six-tap filtering, and Variable Length Coding (VLC). The coded video is abstracted into Video Coding Layer (VCL). To allow network-friendly transport, a Network Abstraction Layer (NAL) decouples coding and compression against transportation. The coded video is then organized into NAL units such that it is mapped effectively according to the underlying transport (e.g. RTP/UDP, H.32X, etc.) [10]. H.264/AVC is primarily distinct with respect to its predecessor (e.g. H.263), in that, there is a well-defined and clearly demarcated specifications for coding and transportation. For instance, VCL and NAL layers effectively improve video coding efficiency by organizing frame units in a hierarchical way as well as by attaching a varying degree of transport importance to them. The NAL non-VCL frames contain important header information for a large number of VCL NAL units and each VCL NAL unit contains samples of video pictures [10]. Thus, any lost video samples can be recovered through inter- and intra-coding techniques and error correcting codes by referring to a specific frame(s) of interest.

Studies [3], [4] have shown that higher video error resilience is achieved when layered coding is combined with transport prioritization. For instance, base layer may contain synchronization headers and basic video samples capable of reconstructing original video using intra-coding, while enhancement layer may carry the differences. A two-layer conditional-replenishment Variable Bit Rate (VBR) video coding and network transportation was studied in detail by Ghanbari in [3]. Here, protection against varying network conditions was achieved by low quantization of high-frequency interframe layer and by diverting some video blocks from enhancement (intraframe) layer to base layer. In [4], the authors studied four MPEG-2 methods for layering video frames including data partitioning, signal-to-noise ratio scalability, spatial scalability, and temporal scalability. Their experimentation revealed that better cell loss resilience with loss rate of 10^{-3} was achieved in all the cases over scalable two-layer encoding and network transport.

In our context, it is thus efficient to offer multilayer voice and video services over IEEE 802.11 with enhanced MAC support. In this new QoS supplement standard to IEEE 802.11 MAC DCF, a single MAC can have multiple classes operating at different priority levels (known as Access Categories) [22]. These access categories define priority levels based on MAC contention window, interframe space, and transmission window opportunities. Higher priority classes gain higher access to the wireless channel. Literatures [7], [12] observed that such an IP-like QoS differentiation at MAC enables support of multimedia services with rigid QoS demands. However, we are unaware of any quantitative study on voice and video streaming over differentiated MAC EDCF using cross-layer techniques. In this paper, we study a two-layer MPEG4 FGS-like video streaming (with concurrent voice conversation streams) over IEEE 802.11e MAC Access Categories for video (AC=1,2). We model MAC using Head-of-Line (HOL) queueing discipline for various access categories.

Because of MAC differentiated services, we naturally expect that base video layer be guaranteed higher access to wireless medium and also be guaranteed higher protection against channel errors. In addition, conversational and streaming services require a tighter time-bound (in the order of few milliseconds) frame reception guarantee. However, studies [23], [12], [11] have shown that such time-bound guarantees are hard to achieve due to: 1) stochastic channel error conditions such as path-loss and fading, 2) time-varying transmission conditions such as number of nodes in the network, and 3) time-invariant MAC layer parameters. To further worsen, the nature of IEEE 802.11e MAC priority discipline is such that higher priority voice and video frames gain higher access to wireless channels. However, there is no higher guarantee of successful transmission of these frames. A quantitative study of this high-priority low-guarantee is established in our report [16]. The peculiar nature of MAC EDCF is due to: 1) large variation in contention window of MAC EDCF binary backoff scheme, 2) smaller range of selection of control window bounds $\{CW_{i,min}, CW_{i,max}\}$, corresponding to priority class i, thus leading to higher collision losses for higher priority classes, and 3) smaller MAC retry limits for higher priority classes to reduce collision resolution delay. It is precisely due to the problem of lower frame transmission guarantee for higher access categories that we argue hybrid ARQ technique at video transport layer will prove to be beneficial over MAC EDCF. In our paper, we demonstrate this through rigorous analytical methods accompanied by a several experiments using in-house MMCP platform.

In addition to channel contention due to MAC binary backoff, varying wireless channel conditions further deteriorate the frame transmission guarantee. This occurs due to several reasons – wireless capture effect, hidden node effect, channel interference, and disturbances caused due to node movement. Further, the wireless channel exhibits stochastic and bursty noise due to multi-path losses and fast fading effects, typically modeled using impulse-response filters [23]. Error concealment schemes such as FEC do not perform well in such bursty noise environments as shown by Chen *et al.* in [24]. In their experiments, packet error rates as worse as 16% does not yield much benefit when FEC additional bit overhead is as good as 50%-75%. In the context of video coding, such frame errors or random losses of NAL non-VCL headers and synchronization units lead to inevitable loss of decoding ability of subsequent video blocks [11]. Thus, we contend that it is not sufficient to provide a completely error-free multilayer video service over IEEE 802.11e without appropriate network or video transport feedback. Given the high-priority low-guarantee nature of MAC EDCF amidst wireless error conditions, we seek techniques to improve frame transmission guarantee at video transport layer. We are intrigued as to how the well-studied type-II ARQ technique with hybrid FEC/ARQ error control and detection can improve the frame transmission guarantee. Specifically, we would like to question if there exists a bounded retransmission delay for frames identified for source video retransmission (at receiver) and if so, can it give clues on the average number of such retransmissions possible, given the video coding rate and the underlying channel conditions?

In recent years, several studies on cross-layer techniques have proven to efficiently transport real-time media over IEEE 802.11 WLAN [9], [13]. Shan *et al.* [9] developed an application-level packetization scheme that decomposes a video frame into integer number of equal-sized link frames. This enabled them to selectively identify and request retransmission of packets (transport protection). To limit video coding delay, they provided application-level packet-based FEC error protection. In [13], Bucciol *et al.* used application-level temporal and perceptual importance of video packets to prioritize and schedule MAC frames for retransmission. The encoder sets a weight appropriate for the MAC frame with respect to its corresponding video frame playback deadline, thus enabling a higher perceptual quality of media. While these cross-layer techniques arguably perform well, we contend that there is sufficient information available at EDCF MAC that can be utilized in video coder/decoder layer, which, along with forward error concealment can provide an error-free and higher frame transmission guarantee. In this paper, we study a new cross-layer technique that makes use of IEEE 802.11e EDCF MAC queueing delay at sender to establish a probabilistic bound for retransmission delay of successfully retransmitting type II frames that are identified as not decodable.

Our broad scheme of things is as follows. In section II, we describe our system model as a two-layer source coding with transport prioritization. We describe the MAC parameters used in analytical and simulations. In section III, we establish MAC contention resolution delay distribution using steady-state collision probabilities under multiple priority levels of voice, video and data frames of IEEE 802.11e EDCF. Our main contributions are: 1) modeling a true *virtual collision handler* at MAC scheduler for video and data priority levels, 2) incorporating a wireless channel error model considering a time-variant Rayleigh slow-fading distribution and studying its effect on MAC EDCF transmissions, and 3) introducing a new cross-layer parameter – expected MAC retries at sender, that is used by video streaming server to schedule new frames for transmission. In section IV, we model video delay over MAC EDCF using Head-of-Line (HOL) priority queueing discipline. We model video queueing delay considering two-layer (base and enhancement layers) arrivals at the video queue along with a concurrent constant-rate single-stream voice conversation. The total MAC EDCF video queueing delay is the sum of expected waiting time of higher priority voice frames waiting to be serviced, plus the service residual of best-effort data and the expected waiting time of video frames that arrived earlier at the HOL queue. Subsequently, we model video retransmission events at receiver as renewal-reward process of

TABLE I
MAC SYSTEM PARAMETERS USED IN MODEL AND SIMULATIONS

MAC Packet payload	1024 bytes
RTS header	20 bytes
CTS header	14 bytes
PHY bit rate	2Mbps
Propogation delay	1 μs
Slot time	50 μs
SIFS	28 μs
DIFS	75 μs
$AIFS_{voice}$	40 μs
$AIFS_{video}$	65 μs
RTS retries	5
CTS timeout	300 μs
ACK timeout	300 μs

TABLE II
RECOMMENDED VALUES FOR MAC EDCF PRIORITY DIFFERENTIATORS

Parameter	0 (Best Effort)	1 (Video Probe)	2 (Video)	3 (Voice)
CW_{min}	31	31	31	7
CW_{max}	1023	1023	63	15
AIFS	DIFS	65 μs	65 μs	40 μs
TXOP	NA	90 μs	90 μs	80 μs
L_{retry}	7	7	7	4

frame(s) identified for retransmission to establish the “spread”-time between successful renewals. The “spread”-time or the inter-arrival time between renewal events is indeed the probabilistic retransmission bound that we seek for a single video frame identified for retransmission. In section V, we verify the analytical bounds using several experiments using our in-house Multimedia Mobile Communication Platform (MMCP) for studying the cross-layer functionalities of IEEE 802.11e EDCF using varying number of nodes for various voice and video frame losses. We perform several two-layer video streaming experiments at MAC-SAP layer and study the video perception quality using PSNR and MOS. We conclude our findings in section VI.

II. SYSTEM MODEL

In this section, we describe our network model and MAC parameters used in our analytical model and simulations. Our network consists of several mobile IEEE 802.11 stations (QSTA) enabled with MAC Enhanced Distributed Coordiation Function (EDCF). Nodes form a closed infrastructure-based Basic Service Set (BSS) network communicating with a single access point (QAP) per BSS, which is also MAC EDCF-enabled. All QSTAs route packets directly through QAP within the BSS network. This forms an single-hop end-to-end network model.

At the network layer, we assume a stable wireless condition: 1) static path between nodes and statibility in routes, 2) nodes do not join or leave during streaming session (simplifies MAC contention model), and 3) bursty wireless channel error conditions due to interference and multipath loss.

For video transport, we choose one among the QSTAs in the BSS as a video streaming broadcast server, while other QSTAs listen. Video streaming is performed at a MAC broadcast level. Further, all stations concurrently initiate a single-stream voice conversation with its neighbor, which is active throughout the video streaming session.

A. IEEE 802.11e MAC EDCF

IEEE 802.11e supports contention-based, contention-free (CF) and hybrid coordination function channel (HCF-based) MAC channel access methods. In this paper, we study contention-based channel access scheme with special attention to evaluate the effect of MAC priority-based channel access on video streaming. The intention is to understand the effectiveness of MAC priority levels in providing rigid demands of application-level quality-of-service. Further, such studies help in identifying appropriate cross-layer parameters required at the application layer.

In Table I, we list the MAC system parameters used in our model and simulations. The values are in accordance to the standards but are chosen suitable for software simulation conditions as well. That is, the relationships between MAC system parameters including slot time, SIFS, DIFS and AIFS are preserved as per the original IEEE 802.11e specifications [22]. Physical layer (PHY) channel capacity is chosen to be 2Mbps. RTS retries define the number of times every MAC frame is attempted before discarding it. This is in addition to the number of retries due to channel collisions.

In IEEE 802.11e, EDCF MAC defines four basic traffic Access Categories (AC) prioritizing voice (AC=3), video, video-probing and best-effort data traffic with decreasing order of priorities. Priorities are defined based on: 1) contention window (CW) minimum and maximum values, 2) arbitrary interframe spacing (AIFS), 3) transmission opportunity window (TXOP), and 4) number of MAC retries. In Table II, we summarize the MAC EDCF Access Categories (AC) parameters used in this paper.

In our model, each MAC node is capable of generating voice, video and best-effort data concurrently. At the MAC-SAP layer, we model these priority classes as queues using Head-of-Line (HOL) queueing discipline. To simplify our model, we consider the video queue in a saturated condition i.e. there is always a video frame ready to be transmitted. This is a reasonable assumption for a continuous real-time broadcast video streaming. In such a transmission system, channel collisions can occur between voice, video and data frames within the node itself and between other communicating nodes in the network. To improve efficiency, our MAC queue scheduler employs a true *virtual collision handler* to resolve internal backoff conflicts among various priority queues. When internal virtual collisions occur, frame with higher priority wins the virtual collision and gets an opportunity to transmit over the wireless medium. In addition to standard IEEE 802.11e, we assume MAC retry count for the number of MAC retransmissions, configurable for each priority class. Note that the MAC retry counts of voice and video frames are kept small but optimum in order to ensure lower transmission delay. The downside of this is higher priority frames being dropped often, as will be observed in later sections.

Finally, we model wireless channel error as a time-varying stochastic noise owing to multipath signal propagation and slow degenerative flat signal fading. We use a two-state Gilbert-Elliott Markov chain model [25], [26] and utilize a Rayleigh fading distribution to model signal strength fading over short distances. This model is then used to study the effects of channel errors on MAC transmissions.

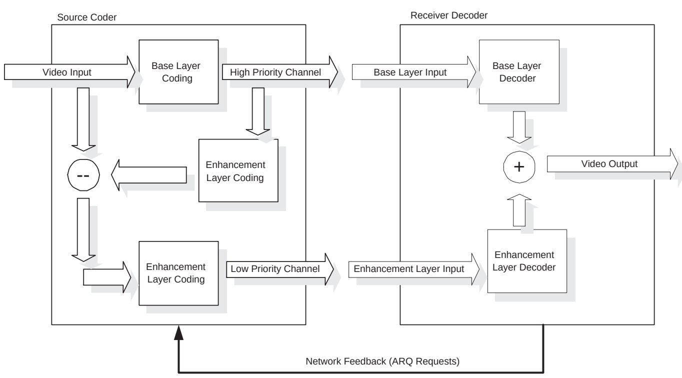

Fig. 1. Two-layer Source Coding and Transport Prioritization.

For modeling video streaming, we consider a two-layer source coding such as MPEG4 FGS – base and enhancement layers. A two-layer coding and transport prioritization is shown in Fig. 1 in which the receiver ARQ feedback is fed back to source for retransmissions. As in the figure, we consider a network model that uses type-II hybrid FEC/ARQ and selective ARQ end-to-end feedback at every MAC node. Each MAC node attempts to retransmit a given frame a finite number of times (given by $L_{i,retry}$) after which the frame is dropped. The base layer is assumed to generate Variable Bit Rate (VBR) frames (but constant bit-rate coded frames) and, the enhancement layer a Variable Bit Rate (VBR) with a variable bit-rate intra-frame coding depending on the available network bandwidth. The justifications of these considerations are explained in later sections.

B. Hybrid FEC/ARQ Models

Early studies on hybrid ARQ models focused on high error-rate satellite channels [1], [2], employing FEC scheme with ARQ protocol. These studies considered Go-Back-N (GBN) or selective ARQ schemes. These and several other studies (not cited here) showed that ARQ by itself leads to throughput degradation if the high channel error condition persists. Under high error conditions, ARQs triggers a large number of retransmission attempts, which in-turn trigger more retransmissions, eventually leading to a complete degradation. Thus, it has been customary to consider ARQ with an error concealment scheme such as FEC. In video streaming, these are type-I and type-II hybrid FEC/ARQ schemes.

Joe [5] studied the performance of hybrid ARQ with concatenated FEC error correction bits in wireless ATM networks in which they adapt the coding rate based on channel conditions using incremental redundancy. Along with this, a high starting coding rate is chosen that enhanced throughput efficiency. Recently, Choi *et al*. [8] developed a hybrid ARQ technique to adapt source coding rate and video frame size based on channel conditions over MAC DCF. Based on the pattern of retransmissions, they observed that it is efficient and practical to retransmit entire type-I or type-II frames, given that decoded errors are found only in some portions of the frames thereby, eliminating the re-coding complexity involved. Several other literatures (not cited here) study the applicability and performance of hybrid FEC/ARQ schemes on ATM wireless networks. We do not summarize them here due to space limitations. We however note that there are only a handful of literatures that study the hybrid FEC/ARQ over IEEE 802.11 WLAN including [8].

Because of the new EDCF-based MAC scheduling policy and due to the complex nature of interaction with other MAC nodes, we find that it is compelling to understand the behavior to effectively model the MAC transmission delay. In this paper, we evaluate video streaming that uses type-II FEC/ARQ source coding over MAC EDCF. We observe in later sections that the inter-ARQ response intervals of video frames at receiver can be modeled probabilistically. Further, the MAC EDCF exhibits interesting and complex interaction with other nodes due to multiple priority levels and due to virtual collisions. These encourage us to study the ARQ behavior over MAC EDCF using cross-layer techniques.

III. Modeling IEEE 802.11e MAC Delay

In this section, we establish the steady-state backoff and collision resolution delay distributions of EDCF MAC queues operating under priority-based scheme. Our analytical model utilizes a 3-tuple discrete Markov chain that represents the EDCF state of MAC node [14]. We assume a finite number of MAC retries after which the frame is dropped. Most importantly, our MAC scheduler implements a true *virtual collision handler* among priority queues thus resolving collisions internally before transmitting frames on the medium.

A. Modeling EDCF Priority Scheme

Consider an IEEE 802.11e EDCF MAC node in which traffic is classified into N priority classes (access categories) $i = 0, 1, \ldots, N-1$. In case of standard IEEE 802.11e, there are four priority classes ($N = 4$) – voice, video, video probe and best-effort data, highest priority being voice. Priority classes are differentiated based on contention window minimum and maximum values, namely $CW_{min}[i]$ and $CW_{max}[i]$ respectively, arbitrary interframe spacing $AIFS[i]$, and the duration of transmission opportunity window $TXOP[i]$, corresponding to priority level i. We define a backoff stage stochastic process $s(i,t)$ of a node at time t as the current transmission attempt of total retransmissions allowed, corresponding to priority level i. Similarly, let $b(i,t)$ be the stochastic backoff counter process that counts backoff time at the beginning of each slot in a node. In their paper, Xiao [14] shows that stochastic process 3-tuple $\{i, s(i,t), b(i,t)\}$ forms a discrete-time Markov chain so long as each MAC frame collides with constant and independent probability. In this paper, we make use of Xiao's [14] 3-tuple model to derive the steady-state contention-resolution delay distribution. Note that a two-tuple $\{s(i,t), b(i,t)\}$ do not sufficiently represent the state space of a Makovian chain. The main difference between Xiao's and earlier models is that the backoff stage process takes values in the range $(0, 1, \ldots, L_{i,retry}-1)$, thus necessarily retransmitting $L_{i,retry}$ times even when the contention window attains the maximum $CW_{max}[i]$. The backoff counter, however, takes values as in previous models, in the range $(0, 1, \ldots, W_{i,j}-1)$, where $W_{i,j}$ represents the current backoff counter, for a given priority level i and a backoff stage j.

Let p_i be the probability that a priority level i MAC node in any backoff stage finds the channel busy.

Under this context, the steady-state probability that a MAC with priority i successfully transmits is given by [14]

$$\tau_i = b_{i,0,0} \times \frac{1 - p_i^{L_{i,retry}+1}}{1 - p_i}, \tag{1}$$

where $b_{i,0,0}$ is the stationary distribution of discrete Markov chain in state $\{i, 0, 0\}$. Let n_i, for $i = 0, 1, \ldots, N-1$, be the number of communicating nodes at each priority level i. Then, probability p_i for a MAC node in any backoff stage to find the channel busy is given by [14]

$$p_i = \begin{cases} 1 - (\prod_{h=0}^{i-1}(1-\tau_h)^{n_h}) & \times \\ & (1-\tau_i)^{n_i-1} \times \\ & (\prod_{h=i+1}^{N-1}(1-\tau_h)^{n_h}). \end{cases} \tag{2}$$

Note that expressions (1), (2) are inter-related with $\tau_i = f(p_i)$ and $p_i = f^{-1}(\tau_i)$, which are then solved numerically. The overall probability p_b that the channel is found busy due to all priority classes is given by [14]

$$p_b = 1 - \left(\prod_{h=0}^{N-1}(1-\tau_h)^{n_h}\right). \tag{3}$$

Similarly, the overall probability p_s that a successful transmission occurs in any given slot due to all priority levels and all communicating nodes is given by [14]

$$p_s = (1 - p_b) \times \sum_{h=0}^{N-1} \frac{n_h \tau_h}{1 - \tau_h}. \tag{4}$$

Using expressions (1)–(4), we now seek to derive the individual probability of finding channel busy due to its own traffic class in a standard IEEE 802.11e MAC. We redefine the notations used earlier such that $p_0 \equiv p_{voice}$ and $p_1 \equiv p_{video}$. The probability that a MAC frame finds the channel busy when it has a voice frame to transmit on the wireless channel is given by

$$p_{voice} = \begin{cases} 1 - ((1-\tau_{voice})^{n_{voice}-1} & \times \\ & (1-\tau_{video})^{n_{video}} \\ & \times(1-\tau_{vp})^{n_{vp}} \times \\ & (1-\tau_{data})^{n_{data}}). \end{cases} \tag{5}$$

Note that even if there are MAC virtual collisions between voice and other frames in the same node, voice frame wins the opportunity to transmit due to higher priority.

For video, probability that a MAC frame finds the channel busy when it has a video frame to transmit on the wireless channel is given by

$$p_{video} = \begin{cases} 1- & ((1-\tau_{voice})^{n_{voice}-1} \times \\ & (1-\tau_{video})^{n_{video}-1} \times \\ & (1-\tau_{vp})^{n_{vp}} \times \\ & (1-\tau_{data})^{n_{data}}), \end{cases} \tag{6}$$

In this paper, we do not derive the channel busy probability for best-effort data.

B. MAC Virtual Collision Handler

In this paper, we model a true *virtual collision handler* at MAC for scheduling of video and best-effort data frames (not applicable for voice). Note that Xiao's model [14] lets the collision occur on the medium itself. While this simplifies the steady-state analysis, we observe that this can lead to significant throughput degradation and elongated video delays at the receiver because: 1) concurrent saturated voice conversation obtains frequent and higher channel access resulting in a greater number of channel collisions between itself and with other nodes and 2) voice frames lost during self-contention inturn queues back in MAC for retransmission thereby elongating channel access to lower priority frames.

In this section, we extend Xiao's model [14] to include a true *virtual collision handler* in which the MAC scheduler internally resolves contention before allowing physical wireless medium access. To achieve this, we assume that the number of MAC retries $L_{i,retry}$, where i represents video and best-effort data priority levels, is the physical collisions on the medium as well as the virtual collisions internally resolved by the handler.

Under this assumption, the 3-tuple Markov chain in Xiao's model [14] will undergo a change in which the non-zero probability from states $\{i, j, 0\}$ to $\{i, j+1, X\}$, where X is any random contention window between $\{CW_{min}, CW_{j+1}\}$, for backoff stage $j+1$. The new non-zero transition probability to the next backoff stage is then given by $(p_i + p_{i,h})/W_{i,j+1}$, where $p_{i,h}$ represents the additional virtual collision probability with respect to all higher priorities. This new virtual collision probability $p_{i,h}$ is given by

$$\begin{array}{rcl} p_{voice,h} & = & 0 \\ p_{video,h} & = & 1-(1-p_{voice})(1-p_{video}) \\ p_{data,h} & = & 1-(1-p_{voice})(1-p_{video})(1-p_{data}) \end{array} . \quad (7)$$

Thus, the probability $\tau_{i,h}$ that a video station transmits during any slot successfully considering internal virtual collision resolution is given from expressions (1) and (7) as below.

$$\tau_{i,h} = b_{i,0,0} \times \frac{1-(p_i + p_{i,h})^{L_{i,retry}+1}}{1-p_i} \quad (8)$$

In later sections, we use (7) and (8) for modeling MAC delay distribution.

C. Channel Error Model

In this paper, we model a time-varying wireless signal strength owing to fluctuations in gain of the channel caused due to multipath signal propagation. Such a signal fading is termed flat fading and typically occurs over short distances when the bandwidth of input signal is narrower compared to the channel coherence bandwidth. Rayleigh fading distribution is the most commonly used flat fading whose probabilistic signal strength PDF is given by [23]

$$p(r) = \begin{cases} \frac{r}{\sigma^2} e^{-\frac{r^2}{2\sigma^2}} & (0 \leq r \leq \infty \\ 0 & (r < 0), \end{cases} \quad (9)$$

where r represents the signal strength and σ is the RMS value of the original signal.

We consider a 2-state Rayleigh fading Markov chain popularly known as the Gilbert-Elliott model [25], [26]. A 2-state model with state and transition probabilitities is described in Fig. 2. We assume that channel bit errors are uncorrelated events and occur independent of each other. This models a slow-varying non-bursty noisy channel.

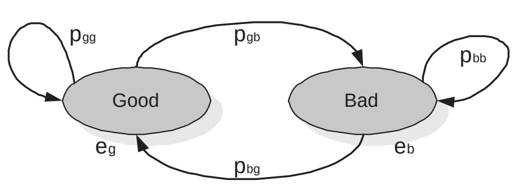

Fig. 2. Two-state Rayleigh fading Markov chain.

Wang *et al.* [27] showed that a K-state Markov chain for any $K \geq 2$ modeled for Rayleigh fading can be optimized with maximum capacity into a 2-state chain such that the average channel error probability e is given by

$$e = e_g \times p_{gb} + e_b \times p_{bg}. \quad (10)$$

In experiments, we observe that for various FEC coding combinations, the packet error rates of e range between 10^{-1} (bad considering FEC) and 10^{-5} (good).

Effect of Channel Error on MAC Transmission

At receiver, the probability of a successful transmission in any given slot due to all priority levels i is given by

$$p_{s,recv} = (1-e) \times p_s. \quad (11)$$

Thus, the probability that a MAC priority queue i successfully transmits is equivalently reduced such that $\tau'_i = (1-e) \times \tau_i$. Correspondingly, the new individual probabilities p'_i of channel being busy for a priority i further deteriorates as p_i is now a function of τ'_i (refer expression (2)).

D. Expected MAC Retries at Sender

We introduce a new cross-layer parameter – the expected MAC retries at sender, that will be used in video transport layer for scheduling new frame transmissions. While deriving this parameter, we consider a noisy channel conditions discussed in the previous section.

Let R_i be the expected number of sender MAC retries for priority level i. Then R_i is given by

$$R_i = \sum_{k=0}^{L_{i,retry}-1} (k+1) \times b_{i,k,0} \times (1-p'_i). \quad (12)$$

Further simplifying (12), we get

$$R_i = \frac{1-p'_i}{p'_i} \times b_{i,0,0} \times \sum_{k=1}^{L_{i,retry}} k \times (p'_i)^k. \quad (13)$$

E. Delay Distribution in IEEE 802.11e EDCF MAC

In this section, we derive the total MAC sender delay including backoff, collision resolution and frame transmission delays. Backoff and collision resolution time in-turn depends on: 1) as many idle slots as backoff counter for each frame retry, 2) as many busy/retransmission slots during which backoff is frozen for each retry, 3) total number of MAC retries for each priority level i, and 4) MAC frame collision delay. Similarly, MAC transmission delay depends on: 1) first IFS delay before backoff is initiated and 2) IFS intervals for successful transmission. For simplicity, we do not consider adjustments in IFS due to the difference in IFS for voice, video and data transmissions. Morever, this paper models only non-TXOP contention-based MAC only.

Given that MAC EDCF chooses contention window values uniformly between $(0, W_{i,j}-1)$, for priority level i and for backoff stage j, the expected number of idle slots that a video frame encounters considering virtual collisions between video-voice and video-data is given by

$$E_{video}[I] = \begin{cases} \sum_{k=1}^{L_{retry,video}} \\ \quad \left(\sum_{j=0}^{k-1} CW_j \times (\frac{p_i'}{W_{i,j}})^j\right) \\ \quad \times(1-p_b) \end{cases} \tag{14}$$

where CW_k is given by

$$CW_k = \begin{cases} 2^k CW_{min}, & k \leq log_2(CW_{max}/CW_{min}) \\ CW_{max}, & k > log_2(CW_{max}/CW_{min}). \end{cases}$$

The expected number of busy slots that a video frame encounters considering virtual collisions is given by

$$E_{video}[B] = \sum_{k=1}^{L_{retry,video}} \left(\sum_{j=0}^{k-1} CW_j\right) \times p_s. \tag{15}$$

Similarly, the expected number of collision slots encountered by a video frame considering virtual collisions is given by

$$E_{video}[C] = \begin{cases} \sum_{k=0}^{L_{retry,video}-1} \\ \quad \left((k+1) \times (\frac{p_i'}{W_{i,j}})^k\right) \\ \quad \times(1-p_b) \times p_s \end{cases} \tag{16}$$

Thus, the overall MAC EDCF frame delay for video is given by summation of expressions (14)-(16). Without considering multiple MAC PDU transmissions, the expected MAC backoff and collision resolution delay is thus given by

$$D_{MAC,video} = \begin{cases} DIFS \times E_{video}[I] + \\ PIFS(E_{video}[B] + E_{video}[C]), \end{cases} \tag{17}$$

where DIFS stands for Distributed Interface Space for idle slots and PIFS stands for PCF Interframe Space for busy and collision slots.

IV. Modeling Video Delay Over MAC EDCF

In this section, we seek to establish average retransmission delay at receiver when video decoder initiates a type-II ARQ request. At receiver, we attempt to bind the average retransmission delay probabilistically, given a constant video coding rate. To achieve these, we first derive the expected waiting time of voice and video frames at sender. We use Head-of-Line (HOL) priority queueing discipline to model the MAC priority queues and derive the average waiting time of voice and video frames. The average waiting time of video frames is the sum of expected waiting time of voice frames, service residual time of best-effort data (lower priority) and the delay incurred in servicing previously-arrived video frames.

Consider the Head-of-Line (HOL) priority queueing discipline at sender as shown in Fig. 3. In HOL, frames are treated strictly on the basis of the access category in which they arrived. Thus, new video arrivals are queued after all voice frames, but before all video probe and before best-effort data frames, and after all previously-arrived video frames. Frames closer to MAC scheduler gets quicker opportunities when compared to those queued behind.

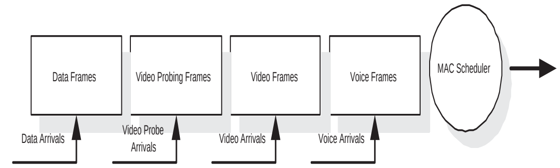

Fig. 3. Head-of-Line (HOL) MAC Priority Queueing.

In order to establish overall waiting time, we must consider: 1) service delay of high-priority voice frames, 2) residual service delay of lower priority non-video frames, and 3) waiting time of video frames awaiting service. We assume a two-layer video streaming over IEEE 802.11e in which the base layer is transported using high-priority queue (AC=2) and enhancement layer (AC=1) using lower-priority queue.

In our model, we assume that nodes are capable of a initiating a single-stream constant-rate voice conversation and also be able to receive a two-layer variable-rate video streams concurrently. The voice stream generated is different from the inline audio streams carried in the MPEG video frames. Voice frames take the the highest MAC transmission priority (AC=3) and hence a minimal support is assumed to study the cross-layer effects on video transmission. We model voice-over-IP using G.711 codec with a coding rate of 64kbps using μ-law encoding. Assuming a fixed voice codec results in a constant voice frame size at every sampling interval. However, it does not guarantee constant arrival rates of voice frames, which is key to queue modeling.

A. Waiting Distribution of Voice

Several earlier literatures [18], [17] studied the probabilistic arrival patterns of voice frames using different codec schemes such as G.711. These studies observed that although voice frame sizes can be fixed for a codec, their inter-arrival rates depend on the codec used and the expected buffer delay. Typically, Pareto, lognormal and uniform distributions are observed to have a closer match to the mean and variance in experiments [17]. In this paper, we choose uniform distribution of voice packet arrivals for the single-stream of voice call as the resultant queueing analysis is simplified. This cumulative distribution $P\{T_{voice} \leq t\}$ of voice frame inter-arrival is given by

$$P\{T_{voice} \leq t\} = \begin{cases} 0, & t < 0 \\ 1, & 0 \leq t \leq T_{voice} \\ 0, & t > T_{voice}, \end{cases} \tag{18}$$

where $T_{voice} = 20$ms is the voice packetization interval for G.711 voice codec. In this paper, we do not intend to study the effect of voice codec and voice arrival rates on the quality of video transmissions.

Before we derive the waiting time distribution of a video frame in HOL, we seek to find the waiting distribution of a voice frame at the high-priority queue. With voice frames arriving with an uniform inter-arrival probability as in (18), we observe that a typical video frame encounters an average of $\lambda_{voice} = 1/T_{voice}$ voice frames per second waiting to be serviced. With the help of Little's theorem, and assuming an exponential service time distribution, we find that the average waiting time of these frames to be serviced is given by

$$E[W_{voice}] = \frac{1}{log(T_{voice})}. \tag{19}$$

We use (19) to derive the overall waiting distribution of video queues in the subsequent section.

B. Waiting Distribution of Video

We model the base-layer video of two-layer coding using MPEG4 FGS as Variable Bit Rate (VBR) arrivals to high-priority MAC AC queue (AC=2). We contend that VBR base layer is well-suited over 802.11e wireless LAN because: 1) VBR base layer carries the least compressible I and P frames and hence require a higher protection, 2) transportation can provide service differentiation and admission control, 3) improve frame transmission guarantee by higher protection through hybrid ARQ/FEC, and 4) enable constant or variable bit rate enhancement layer for bi-directional prediction B-frames. The corresponding enhancement layer is modeled as VBR such that the inter-frame rate is defined as i.i.d. fitting a Gaussian distribution with time-varying mean and variance [6]. Although it is not established strictly that enhancement layer bit rates strictly follow a Gaussian distribution, we still assume so for lack of any better models. Time-varying mean and variance is assumed to favor VCL conditional replenishment and motion-compensated prediction (MCP) coding in latest version of scalable video coding.

In order to establish the MAC queueing delays of voice and video frames, it is essential to understand the MAC service discipline. To do so, we remind ourselves that it is not uncommon to model 802.11 MAC service delay as exponentially distributed [12], [15]. We have discussed the possibility of exponentially distributed service intervals in detail in [15]. In [15], we observe that MAC service interval indeed converge to a known exponential distribution for a network typically with a large number of nodes. Further, we observed that the mean of MAC DCF service distribution converges to the expected service delay between successful transmissions under high contention conditions. In this paper, we assume network and channel contention conditions suitable to apply convergence to exponentially distributed service intervals for MAC EDCF queues.

Next, we model the arrival rates of base layer video frames as VBR arriving at the 802.11e queue with access category (AC=2) queue. We are motivated by the studied on traffic modeling of VBR streams using arriving base and enhancement frame-sizes. In the context of wireless transmission, it is encouraging to model using frame-sizes because a loss of part of I- or P-frames in a GOP results in a considerable degradation and error propagation compared to a B-frame, in which only the frame is affected. Thus, it becomes important to model the sizes of I, P and B frames. Literatures have proposed lognormal [21] and Gamma distributions [19], [20] for modeling these frames. We are motivated to model I- and P-frames as Gamma frame-size distributions as we have observed good correlations to this in our experiments with various video samples [16].

Modeling frame size distribution does not directly yield VBR arrival rates of the video frames unless the codec and video frame rates are fixed. As suggested earlier, we use MPEG4 FGS two-layer model encoded with fixed frame rate (FPS) before transmission. This leads us directly to a Gamma distributed inter-arrival intervals with arrival rate λ_{base} given by

$$P\{1/\lambda_{base} \le t\} = \frac{1}{\beta^{\alpha}\Gamma(\alpha)} \times t^{\alpha-1}e^{-t/\beta}, \tag{20}$$

where the parameters are chosen such that $\beta = 1/(\lambda_{base})^2$ and $\alpha = 1/\lambda_{base}$ and $\Gamma(\alpha) = \int_0^{\infty} t^{\alpha-1}e^{-t}dt$.

The corresponding expected VBR arrival rate of enhancement is λ_{en} with a variance $\sigma^2_{en}(t)$ arriving at access category corresponding to video probing (AC=1). In this paper, we insist on providing higher guarantee and protection to base video layer only.

C. Queueing Delay At Sender

Together with an exponentially distributed service, we now have a G/M/1 priority queueing discipline for the base queueing frame with arrival rate λ_{base} and service μ_{base}. A detailed analysis of G/M/1 queue over MAC EDCF for base and enhancement video frames is available in technical report [16]. Without going into much details, we present the steady-state queue length distribution of G/M/1 queue as below.

$$E[N_{base}] = \frac{\sigma}{1-\sigma}, \text{where } \ \sigma = \frac{\rho^{\alpha}}{(1+\rho)^{\alpha}}, \tag{21}$$

where $\rho = \lambda_{base}/\mu_{base}$ is the expected load of the base frames. The expected waiting time of base frames is thus given by

$$E[W_{base}] = \frac{\sigma}{\lambda_{base}(1-\sigma)}. \tag{22}$$

Thus, the overall waiting time of a typical base video frame is given by

$$E[W_{video}] = E[W_{voice}] + E[W_{base}] + E[W_{en}] \tag{23}$$

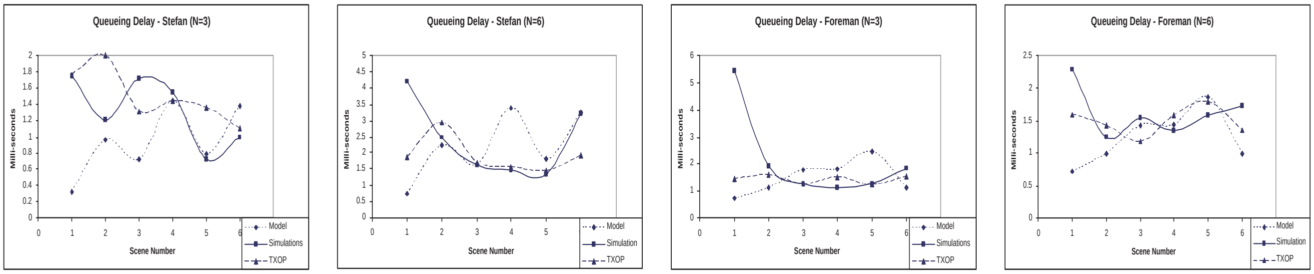

(a) Stefan MP4 Base with N=3

(b) Stefan MP4 Base with N=6

(c) Foreman MP4 Base with N=3

(d) Foreman MP4 Base with N=6

Fig. 4. Queueing Delays of 2 video samples - model versus simulations

Note that, a constant receiver video processing acknowledgement delay further adds to the queueing delay and hence may further degrade the overall video quality.

In Fig. 4, we demonstrate the analytical values obtained from (22), (23) against the simulations for two video samples for N=3 and N=6 number of video nodes respectively. In the same figure, we observe through simulations that one among the N nodes perform MAC-level streaming broadcast to other nodes. All nodes initiate a constant single-stream voice conversation with its neighbor. As seen in the figure, the expected queueing delay for larger sequence of frames (frames 1-3) are significantly higher as shown in the model and correspondingly agreed well in the simulations. These are low-compression I- and P- frames appearing during the inital transmission session. Furthermore, we perform experiments with nodes enabled in TXOP mode (default experiment is setup for EDCF contention mode only). These experiments consistently demonstrate a lower queueing delay for TXOP-enabled nodes owing to the greater access to the channel, as expected. However, TXOP delay is not modeled analytically above.

D. Video Retransmission as Renewal-Reward Process

We model video decoder automatic retransmission request (ARQ) process at the receiver as a renewal-reward process and establish mean “spread”-time (inter-arrival) between successful renewal processes. The “spread”-time is indeed the probabilistic retransmission bound that we seek for a single video frame identified for retransmission.

Consider a two-layer source coding and transport prioritization model as in Fig. 1. At the receiver video decoder, one or more consecutive video macroblocks are detected as undecodable if forward error concealment and type II (previous) undecodable blocks do not yield successful decoding of current blocks. Thus the identified blocks (and all corresponding MAC frames) need to be retransmitted. We define a random counting process $\psi = \{t_n\}$ as a discrete-time renewal sequence for which the interarrival process is i.i.d. defined by $\{R_n\}$. Here, t_n denotes the n^{th} sequence of renewal epoch for which the interarrival distribution is given by $F(x) = P\{R \leq x\}$. The reward process is the reward achieved at every renewal event. In our model, we define the reward process to be same as renewal counting process. In our model, each retransmission request at receiver is considered a renewal event and each successful frame receipt at receiver is considered a reward event.

Because the retransmission renewals are random sequences, the delay between two successful retransmissions is not the difference between the occurrence times of the events. Instead, it is the “spread”-time or the interarrival time between two successful renewals. For any general distribution $F(x)$, the “spread” of renewal sequence $\{R_n\}$ is given by $E[R^2]/E[R] \geq E[R^2]$.

In our case, we seek to derive the “spread” of renewal sequence $\{W_{base,k}\}$ for the overall waiting time plus the video processing time between successful or failed renewal epochs for the k^{th} sequence. Note that we have established $E[W_{video}]$ in (23). We observe that the distribution of delay sequence is exponentially distributed owing to the exponential nature of service interval distribution as observed in earlier section. Thus, the ”spread” of sequence $\{W_{base,k}\}$ is nothing but

$$(E[W_{video}])^2/E[W_{video}] = E[W_{video}]. \qquad (24)$$

That is, the average interarrival delay between successful retransmission epochs is the same as the overall expected MAC queueing, video processing and frame acknowledgement delays. Note that the case is special for exponential distribution as $(E[W_{video}])^2 = E[W^2_{video}]$.

E. Bounds on Retransmission Delays

In this section, we probabilistically bound the retransmission delay obtained in the previous section against a known constant video buffering and coding rate.

Lemma 4.1: For a given video coding and a playout buffer time constant V, ARQ-based retransmission is considered successful if and only if $N_{retransmit} \times E[W_{video}] \leq V$, for any positive non-zero integer $N_{retransmit}$.

Proof: Consider the overall retransmission time distribution $\{W_{base,k}\}$ that includes MAC queueing delay due to backoff and collision resolution, receiver video processing and receiver-initiated acknowledgement delays. We use the well-known Markov inequality principle to bind the expectation of the overall retransmission delay distribution against constant V For a positive video threshold time V, the probability that retransmission delay is smaller than video threshold time is given by

$$Pr\{N_{retransmit} \times |W_{video}| \leq V\} \geq 1 - \frac{N_{retransmit} \times E[|W_{video}|]}{V}. \tag{25}$$

Note that $N_{retransmit} \times E[|W_{video}|]$ in (25) is the overall sample mean of sum of all failed retransmission renewal epochs. Because the left-side of (25) is a probability space, it is bounded by 1 leading to

$$N_{retransmit} \times E[|W_{video}|] \leq V. \tag{26}$$

Thus proved. ■

Intuitively, (26) suggests that the number of allowed ARQ retransmissions is bounded by $V/E[W_{video}]$ and thus, it is a critical criterion to decide if at all retransmission would be effective or not, given a video playout buffer V.

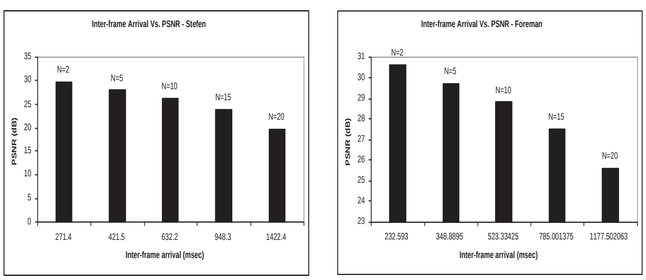

(a) Stefan - Single, Temporal

(b) Foreman - Single, Temporal, Spatial

Fig. 5. Inter-frame Interval and PSNR Degradation without channel losses.

V. Simulations

We validate our analytical model and the bound established above through several experiments on our Multimedia Mobile Communication Platform (MMCP). We used standard VBR traffic from known video YUV sources simulating the base and enhancement layer video traffic. Our topography is 200×200m rectangular 2-dimensional grid with several mobile nodes at random. Nodes operate with a channel capacity of 2Mbps.

A. Multimedia Mobile Communication Platform – MMCP

Our primary motivation to implement Multimedia Mobile Communication Platform (MMCP) is to study the cross-layer effects between MAC, MAC Service Access Point (SAP) and transport. We have implemented IEEE 802.11a/g/e-compatible MAC state engines that exposes well-defined user-APIs to allow to communicate with the MAC. MAC-SAP APIs allow to configure MAC parameters such as retry counts, contention window and TXOP values. Further, the functionality of BSS Access Point (AP) and those of wireless nodes are logically separated API-wise such that users do not have access to the AP-level APIs. The system is entirely written in POSIX-standard C on Windows platform.

TABLE III
VOICE AND VIDEO PARAMETERS USED IN SIMULATIONS

Video codec	MPEG4 FGS two-layer
Single-Temporal	10-12
Temporal-Spatial	(1,4)
Video rate	30 FPS
MTU payload	1024 bytes
Streaming	RTP hinted
Playout buffer	33ms
Voice codec	G.711
Voice bitrate	64kbps
Packetization	20ms

At the backend, each instance of the state engine emulates a wireless node capable of sending and receiving 802.11 MAC control, management and data frames. These are achieved using interprocess and transport socket-layer communications. These MAC nodes use various default values as listed in Table I, II.

For voice and video streaming, an end-to-end encoding, traffic generation at MAC-SAP, decoding and analysis is developed that currently supports MPEG FGS single and two-layer streaming. The framework allows end-users to stream using a server and simultaneously trace the video-quality and perception at 802.11 nodes including PSNR and MOS. Voice and video streaming parameters used in our simulations are listed in Table III.

B. Discussions

We perform several experiments with primarily two video samples – *stefan* and *foreman*. In our experimental setup, one among the BSS nodes act as a streaming broadcast server, while all others listen. Streaming is done at a MAC-level. Simulataneously, all nodes originate a single-stream of voice conversation with their "neighbouring" nodes.

In Fig. 5a and Fig. 5b, we demonstrate the effect of video degradation (through PSNR) as some portions of I- and P-frames are lost during transmissions (owing to higher channel resolution delays). The inter-frame intervals in the figure correspond to those critical frames lost during the transmission. As can be seen, the average interarrival delays of such frames increase with the number of nodes present in the network. Most of these nodes are involved in single-stream voice conversation, while listening to video broadcast

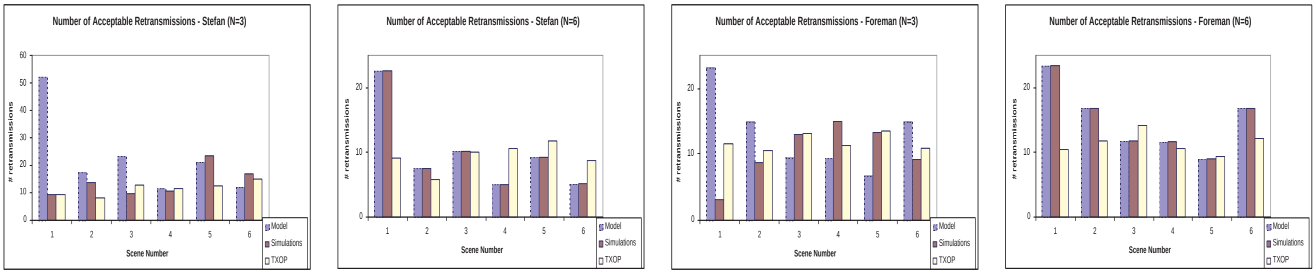

(a) Maximum allowed Retransmissions for $N = 3$ - Stefan

(b) Maximum allowed Retransmissions for $N = 6$ - Stefan

(c) Maximum allowed Retransmissions for$N = 3$ - Foreman

(d) Maximum allowed Retransmissions for $N = 6$ - Foreman

Fig. 6. Acceptable Retransmissions - Stefan and Foreman scenes

streaming. This leads to upto 33% degradation in overall sequence PSNR of the video frames as the number of nodes increases to N=20 for *stefan* with single and temporal frames.

In Fig. 6a – Fig. 6d, we show the finite ARQ retransmission bounds established through analytical model and through experiments with two video samples. The various constant parameters used in simulations are listed in Table I, II. These figures demonstrate the acceptable values of ARQ retransmissions allowed, given the number of nodes and the channel conditions. We perform four sets of experiments with two video samples for N=3 and N=6 respectively. Our immediate observation is that the overall video retransmission delay is bounded for various video nodes, while each voice conversation is still active. We use a video playout buffer of V=33msec in our experiments. The trend in the number of such ARQ retransmissions agree well with our model in (26). Further, we have also performed experiments with and without enabling TXOP in the 802.11e nodes and the difference is significant. As can be seen, the number of ARQ retransmissions acceptable are consistently higher for TXOP-enabled nodes suggesting that they are effective in utilizing the medium. It should be noted that the varying number of nodes effectively varies the wireless channel conditions.

VI. Conclusions and Future Work

In this paper, we established through analytical and real experiments, the retransmission delay bound for transporting layered video over IEEE 802.11e priority MAC EDCF. Most of the other solutions adopt a receiver-based adaptive media playout approach for determining the suitable buffer requirement based on network conditions. In this paper we established a tight retransmission delay bound that is readily adoptable in any delay-sensitive scalable video algorithms. Thus, for a given receiver buffer size and video coding rate, a jitter-free playback can be achieved.

In future, we intend to study video streaming over multihop infrastructure based ESS and as well as mesh networks. Such networks offer significant challenges in terms of modeling the link noise, path and route stability and still be able to provide guarantteed quality of service. On the cross-layer, we intend to model TXOP window opportunities and study the effects of other MAC parameters on quality of voice and voice streaming. We also interested in studying the effects of several concurrent voice streams on the perceived quality of multilayer video streaming.

References

[1] S. Lin and P. S. Yu, “A Hybrid ARQ Scheme with Parity Re-transmission for Error Control of Satellite Channels,” IEEE Trans. Comm., vol. COM-30, pp. 1701-1719, Jul. 1982.

[2] D. Towsley and S. Mithal, “A Selective Repeat ARQ Protocol for a Point to Multipoint Channel,” in Proc. of IEEE INFOCOM 1987.

[3] M. Ghanbari, “Two-layer Coding of Video Signals for VBR Networks,” IEEE J. Select. Areas Comm., Vol. 7, pp. 771-781, Jun. 1989.

[4] R. Aravind, M. R. Civanlar, and A. R. Reibman, “Packet Loss Resilience of MPEG-2 Scalable Video Coding Algorithms,” IEEE Trans. on Circuits and Systems for Video Tech., Vol. 6, pp. 426-435, Oct. 1996.

[5] I. Joe, “An Adaptive Hybrid ARQ Scheme with Concatenated FEC Codes for Wireless ATM,” in Proc. MOBICOM, 1997.

[6] K. Chandra and A. R. Reibman, “Modeling One- and Two-Layer Variable Bit Rate Video,” IEEE/ACM Trans. on Net-working, Vol. 7, Jun. 1999.

[7] D.-J. Deng and R.-S. Chang, “A Priority Scheme for IEEE 802.11 DCF Access Method,” IEICE Trans. Comm., vol. E82-B, no. 1, pp. 96-102, Jan. 1999.

[8] S. Choi and K. G. Shin, “A Class of Adaptive Hybrid ARQ Scheme for Wireless Links,” IEEE Trans. on Vehicular Tech., Vol. 50, No. 3, pp. 777-790, May 2001.

[9] Y. Shan and A. Zakhor, “Cross Layer Techniques for Adaptive Video Streaming Over Wireless Networks,” in Proc. IEEE Int. Conf. on Multimedia & Expo., vol. 1, pp. 277-280, Aug. 2002.

[10] Joint Video Team (JVT) of ISO/IEC MPEG, ITU-T VCEG (ISO/IEC JTC1/SC29/WGII, and ITU-T SG16 Q.6, “Draft ITU-T Recommendation and Final Draft International Stan-dard of Joint Video Specification (ITU-T rec. H.264/ISO/IEC 14 496-10 AVC),” 7th Meeting, Pattaya, Thailand, Mar. 2003.

[11] T. Stockhammer, M. M. Hannuksela, and T. Wiegand, “H.264/AVC in Wireless Environments,” Vol. 13, Iss. 7, IEEE Trans. Circuits and Systems for Video Tech., Jul. 2003.

[12] Y. Xiao, H. Li, and S. Choi, “Protection and Guarantee for Voice and Video Traffic in IEEE 802.11e Wireless LANs,” in Proc. of IEEE INFOCOM 2004.

[13] P. Bucciol, G. Davini, E. Masala, E. Filippi, and J. C. De Martin, “Cross-layer Perceptual ARQ for H.264 Video Streaming Over 802.11 Wireless Networks,” in Proc. of IEEE GLOBECOM, 2004.

[14] Y. Xiao, “Performance Analysis of Priority Schemes for IEEE 802.11 and IEEE 802.11e Wireless LANs,” IEEE Trans. on Wireless Comm., Vol. 4, No. 4, Jul. 2005.

[15] S. G. Sitharaman, “Modeling Queues Using Poisson Ap-proximation in IEEE 802.11 Ad-Hoc Networks,” In Proc. 14th IEEE Workshop on Local and Metropolitan Area Networks, Chania, Crete, Greece, Sep. 2005.

[16] S. G. Sitharaman and K. M. Anantharaman, “Impact of Retransmission Delays on Multilayer Video Streaming over IEEE 802.11e Wireless Networks,”, Wipro Technical Report, Aug. 2006.

[17] M. J. Fischer and D. M. Masi, “Voice Packet Arrival Models and Their Effect on Packet Performance,” Applied Telecommunications Symposium. Apr., 2005.

[18] K. Sriram and W. Whitt, “Arrival Processes in Packets Multiplexers for Voice and Data,” IEEE Journal on Sel. Areas in Comm., Vol. SAC-4, No. 6, pp. 833846, Sep. 1986.

[19] U. K. Sarkar, S. Ramakrishnan, and D. Sarkar, “Modeling Full-Length Video Using Markov-Modulated Gamma-Based Framework,” IEEE/ACM Trans. on Networking, vol. 11, Aug. 2003.

[20] M. Frey and S. Nguyen-Quang, “A Gamma-based framework for modeling variable-rate MPEG video sources: The GOP GBAR model,” IEEE/ACM Trans. Networking, vol. 8, Dec. 2000.

[21] M. Krunz and S. K. Tripathi, “On the Characterization of VBR MPEG Streams,” Proc. of ACM SIGMETRICS, vol. 25, June 1997.

[22] *Draft Supplement to Part II: Wireless Medium Access Control (MAC) and physical layer (PHY) specifications: Medium Access Control (MAC) Enhancements for Quality of Service (QoS)*, IEEE 802.11e/D5.0, Jun. 2003.

[23] Theodore S. Rappaport, *Wireless Communications: Principles and Practice*, 2nd ed. Prentice Hall PTR, Dec. 2001.

[24] L.-J. Chen, T. Sun, M. Y. Sanadidi, and M. Gerla, “Improving Wireless Link Throughput via Interleaved FEC,” In Proc. of 9th IEEE Symposium on Computers and Communications (ISCC), Alexandria, Egypt, 2004.

[25] E.N. Gilbert, “Capacity of a burst-noise channel,” Bell Syst. Tech. J. 39 (1960) 1253-1265.

[26] E.O. Elliott, “Estimates of error rates for codes on burst-noise channels,” Bell Syst. Tech. J. 42 (1963) 1977-1997.

[27] H. Wang and N. Moyaeri, “Finite-State Markov Channel - A Useful Model for Radio Communication Channels,” IEEE Trans. Veh. Tech., vol.44, pp. 163-171, Feb. 1995.